# ASSESSMENT OF HARMONICS AND INTER-HARMONIC OF GRID-INTERACTIVE SYSTEMS

**Adjei-Saforo Kwafo Edmund[1,2], Misbawu Adam[1], Solomon Nchor Akansake[3] ,Samuel Addo Darko[1]**

[1]*Faculty of Engineering and Technology, Kumasi Technical University, Kumasi*

[2]*Faculty of Computer and Electrical Engineering,COE, KNUST, Kumasi.*

[3]*Faculty of Physical Sciences Computational Sciences,COS, KNUST, Kumasi.*

## *Abstract*

*Power quality is at all times an important issue in the area of power systems. With the reconstruction of industrial structure and not-long-ago development of intelligent grid technology, more and more renewable energy is integrated into the power systems that may corruptly abase the power quality transmitted to the end-users. Many modern solid-state devices widely used in a range of applications in these green or renewable energy systems offer economical and reliable solution for effective and efficient control of these systems. Notwithstanding these, they also present nonlinear operational characteristics and introduce voltage and current contamination such as harmonics and inter-harmonics into the power grid . The inter-harmonics produced by converters employed in renewable systems are overlooked by some researchers, but their integral effects are very titanic. In this paper, harmonic and inter-harmonics generated by converters used in photovoltaic and wind turbine are investigated. It analyzes the harmonics and inter-harmonic generated by pulse width Modulation (PWM) modulation, the dead zone effects of semi-conductor switching device - Insulated Gate Bipolar Transistor (IGBT), and the DC voltage fluctuations. This leads to observation that as the number of harmonics increases, the switching frequency increases, which has been verified by theoretical analysis, simulation, and experimental results.*

**Keywords:** *Harmonics, inter-harmonics, inverters, photovoltaic*

## 1.0 INTRODUCTION

Recently, renewable energy sources for electric power generation have been drawing more attention from researchers. Many developing countries have resorted to this form of power generation, since resources such as fossil fuel, coal and gas are depleting at a fast rate. The utilization of renewable energy for propulsion and electrification of equipment in a ship is proposed in reference [1-4]. A photovoltaic (PV) energy conversion system fault detection scheme and hybrid dynamic model of marine power where energy storage device is infused to a traditional nautical power plant is presented in [5, 6]. The automotive industry is also focusing on renewable energy sources to enhance system efficiency by minimizing fossil fuel consumption. These resources may also provide better solutions to reducing greenhouse emissions. However, the uncertainties in renewable energy sources such as wind speed and solar irradiance lead to variation in power generation. Therefore, the quality of power by renewable energy source needs to be taken into consideration

for smooth operation in transportation, domestic and commercial power systems. Conventional techniques are being used in marine transportation systems for electric power generation. PVs and wind turbines use inverters to convert the DC to AC to be connected to the grid. Harmonic generated by these inverters due to proportional integral (PI) based on pulse width modulation (PWM) with a large number of power electronic devices exhibit high frequency characteristics. Dead zone effects due to delay in turn on and off of the switches and inter-harmonics due to the DC voltage fluctuations affect power quality of grid. Therefore, it is necessary to study and assess the harmonic characteristics to find a solution so that power quality issues will be improved [7,8].

Several harmonic mitigation methods have been proposed for the mitigation of harmonic distortions [9]-[11]. In references [12]-[14], a medium voltage drive solution adapting front-end current source converters, mitigation of harmonic contamination in multi-bus electrical grid of nautical vessel employs an active power filter. However, the harmonic generation principles of the power electronic devices are not thoroughly analyzed. This paper presents the assessment of harmonic generated in photovoltaic (PV) and wind turbine inverters. Experimental setups and simulations are used to prove the theoretical analysis of the work.

## 2.0 GENERATION OF HARMONIC BY DEAD ZONE EFFECT OF SWITCHING DEVICES

Considering phase A of a two-level three-phase inverter as an example, with reference to the distinct pattern of switching, each phase of the inverter as depicted in Figure 1(a) possesses bi-operating statuses that are donated by letter "P" and "N". An indication of "P" indicates device $VT_1$ is forward bias and $VT_2$ is reversed bias, that is, $U_{dc}$ is the output voltage. This means that the current $i_a$ flows out of the bridge as positive current. Again, an indication of "N" means that the device $VT_1$ is in blocking mode and device $VT_2$ is forward bias, and $U_{dc}$ is zero. This also means that the current $i_a$ flows in the bridge as negative current.

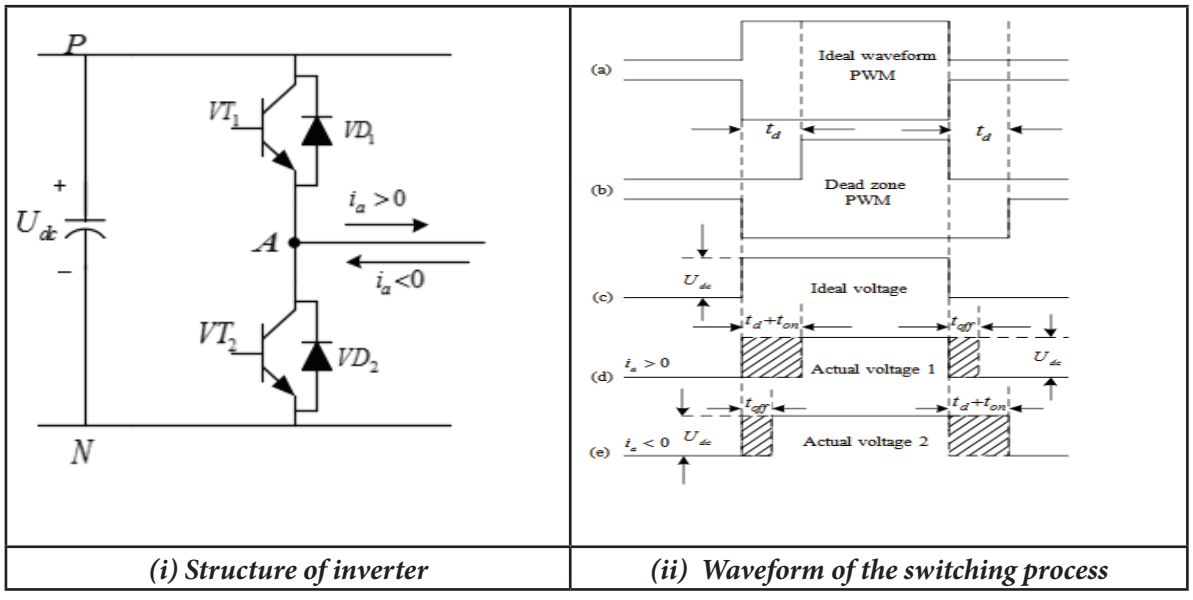


*(i) Structure of inverter* *(ii) Waveform of the switching process*

***Figure 1: Phase-A of a two-level three-phase inverter***

When $i_a > 0$, the dead zone appears at two toggling positions. At first cycle, $VT_1$ is conducting, $VT_4$ is blocked, and $VT_1$ is blocked, $VT_4$ is conducting on during the second half cycle. By analyzing the circuit above and considering the current through the freewheeling diode during the two switching moments, the actual voltage is obtained as depicted in Figure 1(i). At the same time, when $i_a < 0$, the real voltage is displayed in Figure 1(i)(e).

In Figure 1(ii), $t_d$ is the dead time, $t_{on}$ is the turn on time, $t_{off}$ is the turn off time, and $U_{dc}$ is the DC bus voltage. It can be observed from the above analysis that the actual output voltage is distinct from the original output voltage by a pulse voltage error. Using the equal area criterion technique, the mean voltage error can be obtained as

$$\Delta uAN = \begin{cases} f_c T_d U_{dc} & i_a > 0 \\ -f_c T_d U_{dc} & i_a < 0 \end{cases}, \qquad (1)$$

where $T_d = t_d + t_{on} + t_{off}$ and $f_c$ are the carrier frequency.

The distorted voltage is determined by Fourier Decomposition Theorem of the voltage error formed by the dead time. $U_{Tdh}$ is the low harmonic voltage of the inverter and can be calculated as [15]:

$$U_{Tdh} = \frac{4 f_c T_d U_{dc}}{n\pi} \sin n(\omega_r t - \varphi), \qquad n = 3,5,7\cdots \qquad (2)$$

Therefore, the harmonic voltage produced by the effects of dead zone from equation (2) is mainly low, such as 3rd, 5th, 7th and 9th. The switching device dead time is usually a few microseconds. Only when the switching frequency ($F_{SW}$) is high, the dead time takes a long time in one switching cycle, and then the dead zone effect is more obvious. The simulation results shown in Figure 2 are obtained when the dead time is set to 6μs. It can also be observed that when the switching frequency is set to 10 kHz, the presence of dead time causes significant increase in the 5th and 7th order harmonics. However, when the switching frequency is set to 2 kHz, the dead time takes up a small proportion of the switching period, and the effects of dead zone on harmonic generation are insignificant. Therefore, for a high-power inverter, where the switching frequency is low, generally between 1000Hz and 3000Hz, the harmonic produced by the dead zone effect is negligible.

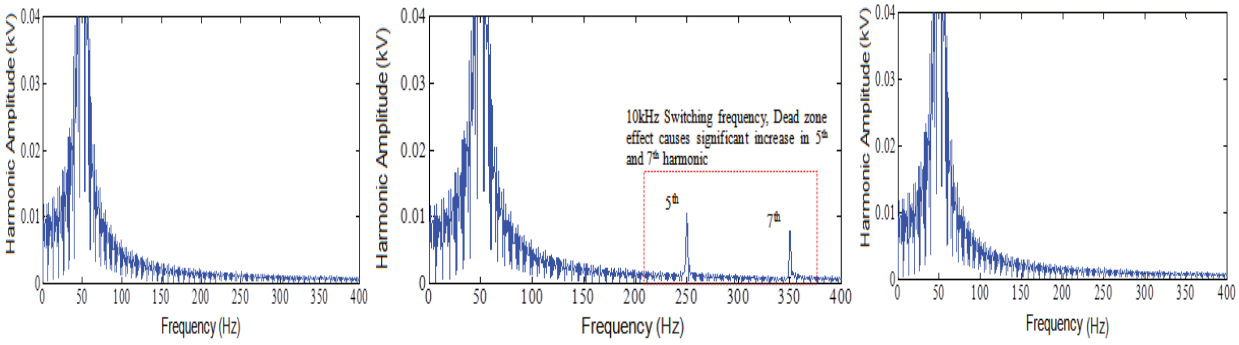


***(a) $F_{SW}$ of 10 kHz, without dead time*** ***(b) $F_{SW}$ of 10 kHz, with dead time of 6μs*** ***(c) $F_{SW}$ of 2 kHz, with dead time of 6μs***

***Figure 2: Effect of dead time on inverter voltage characteristics***

## 3.0 GENERATION OF INTERHARMONICS

Interharmonics are harmonics that are not integer multiple of the fundamental frequency at which the supply system is operating (50/60 Hz) [11]. These phenomena are quickly becoming a problem in power systems due to the extensive increase in the interharmonic producing loads. A source of interharmonic is a static converter switching not synchronized to the power system frequency. Thyristors which are used in these devices are synchronized to the power system frequency during turn off at the same voltage, and therefore do not produce interharmonics. However, thyristors are replaced in converters by IGBT due to their greater flexibility in regulating reactive and as well as real power and damping of power system oscillation. The asynchronous switching of the converters using IGBTs produces interharmonics. For an inverter with PWM modulation, when the DC voltage fluctuates, the AC side of the inverter produces interharmonics [15].

The loads that mainly induce interharmonics include but not limited to voltage source converters, cycloconverters, static frequency converters, arc furnaces, induction motors, variable load drives, power line communications. The periodic fluctuation component, which is generated by DC side voltage of an inverter is given by

$$u_d = U_d \sin(\omega_d t + \phi_d) \tag{3}$$

Considering the SPWM according to the previous analysis, the harmonic component $U_{ab(ih)}$ of the inverter output voltage can be obtained as follows:

When *n=1, 3, 5… m* is an even number of integer multiples of 3,

$$U_{ab(ih)} = \sum_{m=1}^{\infty}(-1)^{\frac{m+1}{2}}\frac{4U_d}{n\pi}\sum_{n=2}^{\infty}J_n\left(\frac{n\pi m}{2}\right)\cdot\sin\frac{n\pi}{3}\cdot$$
$$\left\{-\frac{1}{2}\cos\left[(m\omega_c + n\omega_r + \omega_d)t + n\left(\varphi - \frac{\pi}{3}\right) + \varphi_d\right] + \frac{1}{2}\cos\left[(m\omega_c + n\omega_r - \omega_d)t + n\left(\varphi - \frac{\pi}{3}\right) - \varphi_d\right]\right.$$
$$\left.+\frac{1}{2}\cos\left[(m\omega_c - n\omega_r + \omega_d)t + n\left(\varphi - \frac{\pi}{3}\right) + \varphi_d\right] - \frac{1}{2}\cos\left[(m\omega_c - n\omega_r - \omega_d)t + n\left(\varphi - \frac{\pi}{3}\right) - \varphi_d\right]\right\} \tag{4}$$

When *n=2, 4, 6… m* is an odd number of integer multiples of 3,

$$U_{ab(ih)} = \sum_{m=2}^{\infty}(-1)^{\frac{m}{2}}\frac{4U_d}{n\pi}\sum_{n=1}^{\infty}J_n\left(\frac{n\pi m}{2}\right)\cdot\sin\frac{n\pi}{3}\cdot$$
$$\left\{\frac{1}{2}\sin\left[(m\omega_c + n\omega_r + \omega_d)t + n\left(\varphi - \frac{\pi}{3}\right) + \varphi_d\right] - \frac{1}{2}\sin\left[(m\omega_c + n\omega_r - \omega_d)t + n\left(\varphi - \frac{\pi}{3}\right) - \varphi_d\right]\right.$$
$$\left.-\frac{1}{2}\sin\left[(m\omega_c - n\omega_r + \omega_d)t + n\left(\varphi - \frac{\pi}{3}\right) + \varphi_d\right] + \frac{1}{2}\sin\left[(m\omega_c - n\omega_r - \omega_d)t + n\left(\varphi - \frac{\pi}{3}\right) - \varphi_d\right]\right\} \tag{5}$$

According to equations (4) and (5), the harmonic frequency of the harmonic components caused by voltage fluctuations on the DC side is $(m\omega_c \pm n\omega_r) \pm \omega_d$. That is, the offset occurs at the frequency of harmonic generated by PWM modulation. To prove the affirmation of the above analysis, an AC of 40 Hz frequency is added to the simulation based on the DC voltage. The FFT analysis results of the output voltage waveform of the inverter are shown in Figure 3. It can be observed that the simulation results are consistent with the theoretical analysis results.

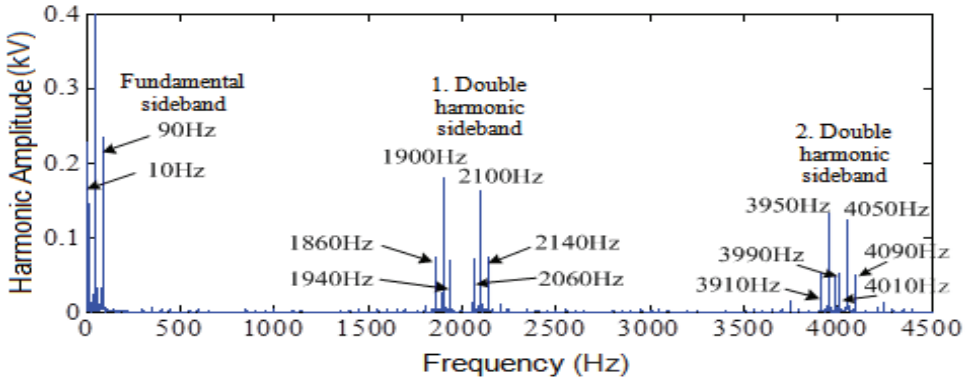


*Figure 3: FFT analysis of inverter output voltage fluctuation*

## 4.0 GENERATION OF HARMONICS IN GRID-INTERACTIVE INVERTER

The schematic diagram of the PV/wind turbine power generation system is shown in Figure 4. During conversion from DC to AC, when PWM is used to control the inverter, high frequency harmonics are generated. In addition, the grid side inverter or interactive inverter generates a certain amount of harmonics that also affects the grid power due to the effect of the dead zone on the toggling components.The harmonics produced by the PV inverter is mainly caused by the PWM switching modulation. The widely used PWM modulation in practical engineering is the sinusoidal pulse width modulation (SPWM). This is due to the fact that it is simple, reliable and a mature technology.

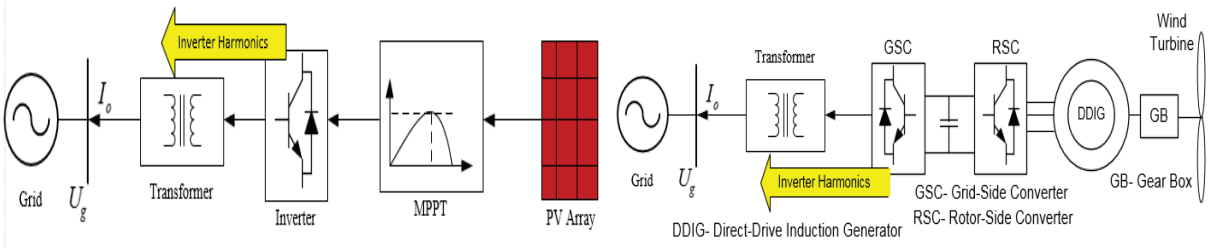


(a) (b)

*Figure 4: Schematic diagram of (a) PV and (b) DDIG power generation systems*

By performing Fourier analysis on the output line voltage $U_{ab}$ of the inverter, the voltage components are given as:

$$U_{ab1} = \frac{\sqrt{3}}{2} M U_{dc} \sin\left(\omega_r t + \varphi + \frac{\pi}{3}\right) \quad (6)$$

Where $U_{ab}$ is the DC side voltage, $M$ is the modulation index, and $\omega_r$ is the modulation wave angular frequency. When the carrier frequency is $\omega_c$, the line voltage harmonics is categorized into the following cases.

**A. Case 1:** The harmonic with old components

$$U_{abh}=\sum_{m=1}^{\infty}(-1)^{\frac{m+1}{2}}\frac{4U_{dc}}{m\pi}\sum_{n=2}^{\infty}J_n\left(\frac{m\pi M}{2}\right)\times\sin\left[\left(m\omega_c\pm n\omega_r\right)t+n\left(\varphi-\frac{\pi}{3}\right)\right]\sin\frac{n\pi}{3} \quad (7)$$

When *n=1, 3, 5…* *m* is an even number of integer multiples of 3, the frequency is $m\omega_c \pm n\omega_r$.

**B. Case 2:** The harmonic with even components

$$U_{abh}=\sum_{m=2}^{\infty}(-1)^{\frac{n}{2}}\frac{4U_{dc}}{m\pi}\sum_{n=1}^{\infty}(-1)^{n}J_n\left(\frac{m\pi M}{2}\right)\times\cos\left[\left(m\omega_c\pm n\omega_r\right)t+n\left(\varphi-\frac{\pi}{3}\right)\right]\sin\frac{n\pi}{3} \quad (8)$$

When *n=2, 4, 6…* *m* is an odd number of integer multiples of 3, the frequency is $m\omega_c \pm n\omega_r$, where $J_n$ is the first class Bessel functions, subscript *n* is the order.

### *4.1 Simulation Using Pscad Software*

Considering the above equations, the corresponding high harmonic content is commonly used for switching frequencies of the converter can be calculated as shown in Table 1. An SPWM simulation model was built in PSCAD simulation software. The DC side voltage of the model was set to 800V; the carrier frequency was set to 2 kHz; and the modulation index was set to 0.9. The simulation result of the line voltage output when the inverter switching frequency is set to 2 kHz is shown in Figure 5. The signal with high harmonics contents are 38$^{th}$, 42$^{nd}$, 79$^{th}$, and 81$^{st}$. It can be observed that the simulation results are consonant with the theoretical analysis results. The comparison of the simulation results of the harmonic amplitude voltage generated by the theoretical calculation and SPWM modulation results of equations (7) and (8) is shown in Figure 6.

**Table 1: Switching frequencies and their corresponding harmonic orders**

| Switching Frequencies(kHz) | High harmonic contents |
|---|---|
| 1.5 | 28、30、59、61 |
| 2.0 | 38、42、79、81 |
| 6.4 | 126、130、255、257 |
| 10.0 | 198、202、309、401 |

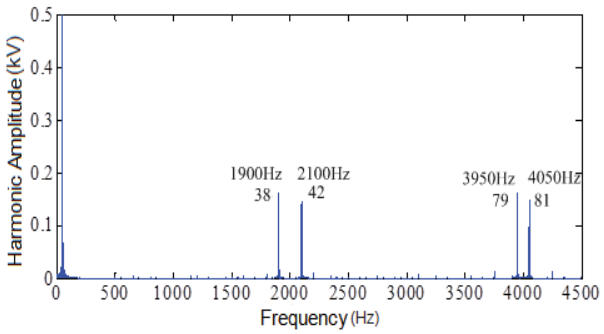


**Figure 5: FFT Analysis of SPWM modulated harmonic line voltage**

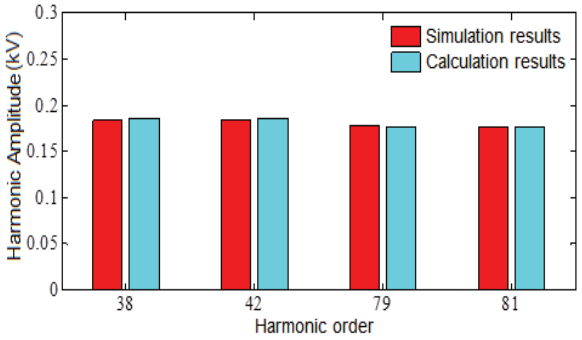


**Figure 6: Comparison between simulation and calculated results of SPWM harmonic amplitude**

## *4.2 Experiment on PV Inverter*

In an experiment, the photovoltaic inverters were taken as the research objects. The inverter power transmission, control parameters, filter structure, grid voltage imbalance and other factors were considered and the effects of the output harmonics have been analyzed.Again, however, the data analysis of the effects of photovoltaic inverter on power output harmonic characteristics and influence of control strategy on harmonic characteristics are analyzed. Carrier frequency is set to 2.5 kHz. Measurement points are selected and defined as shown in Figure 7. The experimental conditions are given in Table 2.

Figure 8 shows the bridge arm inverter output voltage waveform and its FFT analysis. From the FFT analysis, the output voltage harmonics are mainly concentrated around 2500 Hz ($46^{th}$, $48^{th}$, $52^{nd}$, and $54^{th}$), 5000 Hz ($95^{th}$, $99^{th}$, $101^{st}$, and $105^{th}$), which is in line with the theoretical analysis of the harmonic law of SPWM modulation. It should be noted that, because the bridge arm inverter voltage data provided by the manufacturer is insufficient (only 1996 sampling point data), the accuracy of the voltage harmonic amplitude obtained by using the MATLAB software by the fast Fourier algorithm will also be insufficient to provide basis for the model validation. Therefore, the following data verification is mainly based on the bridge arm voltage harmonic data measured by the power quality analysis and the inverter output current and voltage harmonic data measured by the power analyzer.

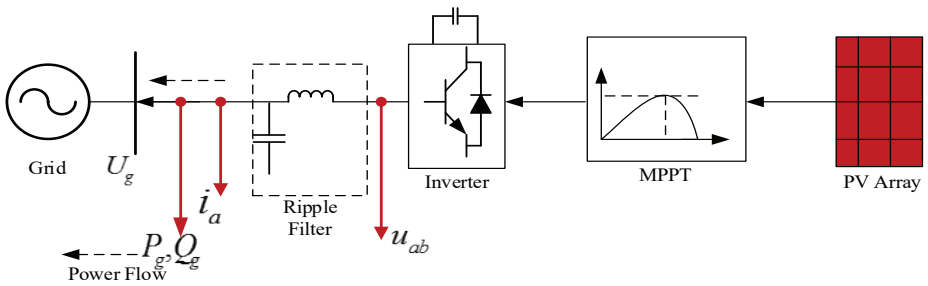


*Figure 7: PV testing wiring diagram*

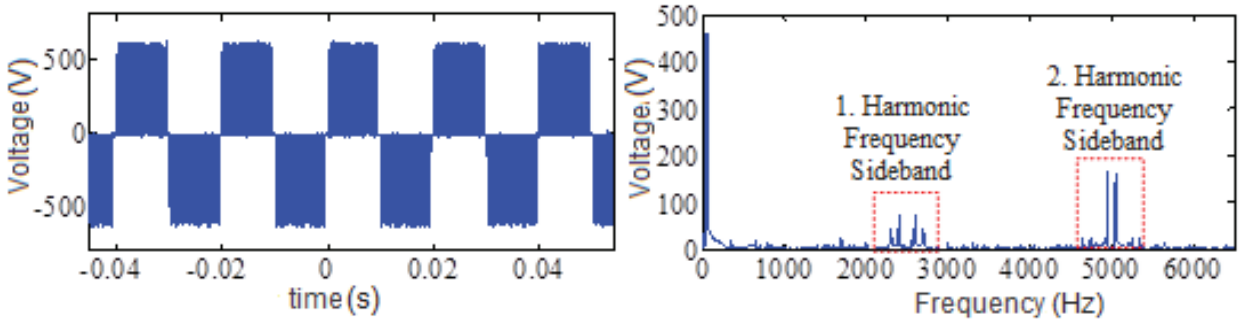


*(a) Voltage waveform* *(b) FFT analysis*

***Figure 8: Bridge arm inverter output voltage***

Figure 9 shows the inverter output current harmonic data measured by the power analyzer. From the data provided, the following observations can be made: (1) The higher harmonics of the inverter output are mainly 46$^{th}$, 48$^{th}$, 52$^{nd}$, 54$^{th}$, 95$^{th}$ and 99$^{th}$, which are located near the carrier frequency and consistent with theoretical analysis; (2) The inverter output lower-order harmonics with larger amplitudes are mainly odd harmonics of 3$^{rd}$, 5$^{th}$, and 7$^{th}$ and even harmonics of 2, 4, and 6$^{th}$, and DC offset are significant; and (3). In the inverter output current harmonics, apart from the harmonics near the carrier frequency and lower harmonic orders, the 17$^{th}$ - 20$^{th}$ harmonic amplitudes are also high. This may be caused by the LC filter resonance, considering the resonance frequency of the filter (L=0.12 *m*H/ph., C=1200 *u*F) and transformer leakage inductance (30 *u*H), is about 937 Hz.

**Table.2. Experimental condition data sheet**

| Site environment | | |
|---|---|---|
| Ambient temperature | | Relative humidity :Good |
| Altitude: less than 1000 meters | | Ventilation conditions: Good, but no air conditioning in the distribution room |
| Test Instruments and parameter settings | | |
| Measurement frequency: 50 Hz | | Nominal input voltage: 400V |
| CT ratio: 800:1 | | VT(PT)ratio: 1:1 |
| Research content | Influence of control strategy on harmonic characteristics | |
| Working condition | kp | ki |
| Working condition1 | 500 | 100 |
| Working condition2 | 500 | 400 |
| Working condition3 | 500 | 800 |
| Working condition4 | 1000 | 100 |
| Working condition5 | 1500 | 100 |
| Research content | Harmonic characteristics based on the power generation output unit | |

| Working condition | Active power (kW) | reactive power (kVar) |
|---|---|---|
| Working condition1 | 150 | 0 |
| Working condition2 | 150 | 120 |
| Working condition3 | 150 | 260 |
| Working condition4 | 300 | 0 |
| Working condition5 | 390 | 0 |

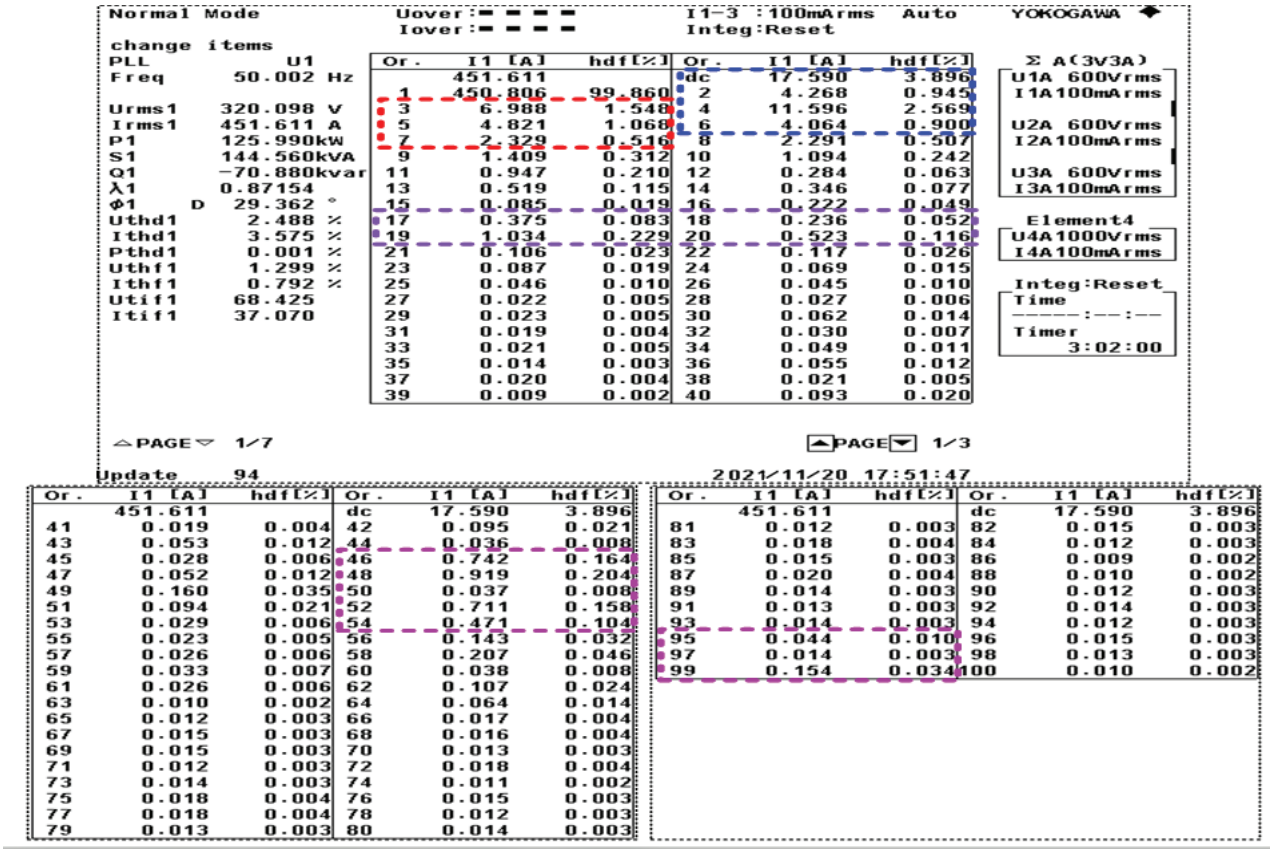


*Figure 9: Inverter output current harmonics data*

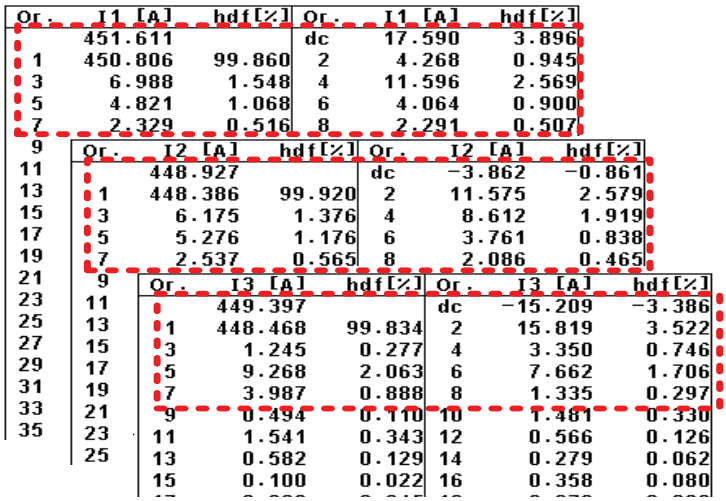

| Or. | I1 [A] | hdf[%] | Or. | I1 [A] | hdf[%] |
|---|---|---|---|---|---|
| | 451.611 | | dc | 17.590 | 3.896 |
| 1 | 450.806 | 99.860 | 2 | 4.268 | 0.945 |
| 3 | 6.988 | 1.548 | 4 | 11.596 | 2.569 |
| 5 | 4.821 | 1.068 | 6 | 4.064 | 0.900 |
| 7 | 2.329 | 0.516 | 8 | 2.291 | 0.507 |

| Or. | I2 [A] | hdf[%] | Or. | I2 [A] | hdf[%] |
|---|---|---|---|---|---|
| | 448.927 | | dc | -3.862 | -0.861 |
| 1 | 448.386 | 99.920 | 2 | 11.575 | 2.579 |
| 3 | 6.175 | 1.376 | 4 | 8.612 | 1.919 |
| 5 | 5.276 | 1.176 | 6 | 3.761 | 0.838 |
| 7 | 2.537 | 0.565 | 8 | 2.086 | 0.465 |

| Or. | I3 [A] | hdf[%] | Or. | I3 [A] | hdf[%] |
|---|---|---|---|---|---|
| | 449.397 | | dc | -15.209 | -3.386 |
| 1 | 448.468 | 99.834 | 2 | 15.819 | 3.522 |
| 3 | 1.245 | 0.277 | 4 | 3.350 | 0.746 |
| 5 | 9.268 | 2.063 | 6 | 7.662 | 1.706 |
| 7 | 3.987 | 0.888 | 8 | 1.335 | 0.297 |
| 9 | 0.494 | 0.110 | 10 | 1.481 | 0.330 |
| 11 | 1.541 | 0.343 | 12 | 0.566 | 0.126 |
| 13 | 0.582 | 0.129 | 14 | 0.279 | 0.062 |
| 15 | 0.100 | 0.022 | 16 | 0.358 | 0.080 |

***Figure 10: Comparison of low-order inverter output current data of a balanced three-phase grid***

In the second part of the above analysis, the test report given by the manufacturer indicates that the inverter itself has a large 2nd, 4th, and 6th harmonic due to control reasons. Figure 11 shows the comparison of low-order harmonic of the inverter output current in a balanced three-phase grid. It can be seen from the figure that 2nd, 3rd, 4th, 5th, 6th and 7th harmonics are shown. The amplitude and DC components have obvious three-phase asymmetry. Therefore, it can be said that the inverter control software may have certain defects, which may cause these low-order harmonics to be excessive. On the other hand, the grid side AC power supply may also generate low-order harmonics, which will have an impact on the output harmonics of the inverter. This is the analysis of influence that the control strategy has on harmonic characteristics of the inverter.

The influence of power output harmonic characteristics is also analyzed. Comparison between working conditions 1, 2 and 3, when the active power is fixed at 150kW and the reactive power is increased sequentially. Considering that some of the characteristic harmonic components are small, 48th, 52nd, and 99th order voltage harmonic is extracted here as reference. The three-phase voltage characteristic harmonic components are shown in Table 3. According to theory, when the active power is kept constant, the modulation index M increases as the reactive power increases. Therefore, the following conclusions can be made from the data presented in Table 3. As the modulation index M increases, the 48th and 52nd order harmonic amplitude increases, however the 99th order harmonic amplitude shows a decreasing trend. The comparisons of the variation in the harmonic orders between respective phases with regard to the working conditions in Table 2 have been clearly illustrated in Fig.12. This condition is consistent with the theoretical analysis.

**Table 3: Voltage characteristic harmonic orders at working condition 1, 2, and 3**

| Voltage | 48th | | | 52nd | | | 99th | | |
|---|---|---|---|---|---|---|---|---|---|
| | A | B | C | A | B | C | A | B | C |
| Condition:1 | 1.244 | 1.318 | 1.268 | 1.081 | 1.151 | 1.091 | 0.485 | 0.575 | 0.501 |
| Condition:2 | 1.384 | 1.486 | 1.436 | 1.22 | 1.326 | 1.247 | 0.442 | 0.517 | 0.463 |
| Condition:3 | 1.56 | 1.653 | 1.613 | 1.367 | 1.47 | 1.391 | 0.364 | 0.437 | 0.385 |

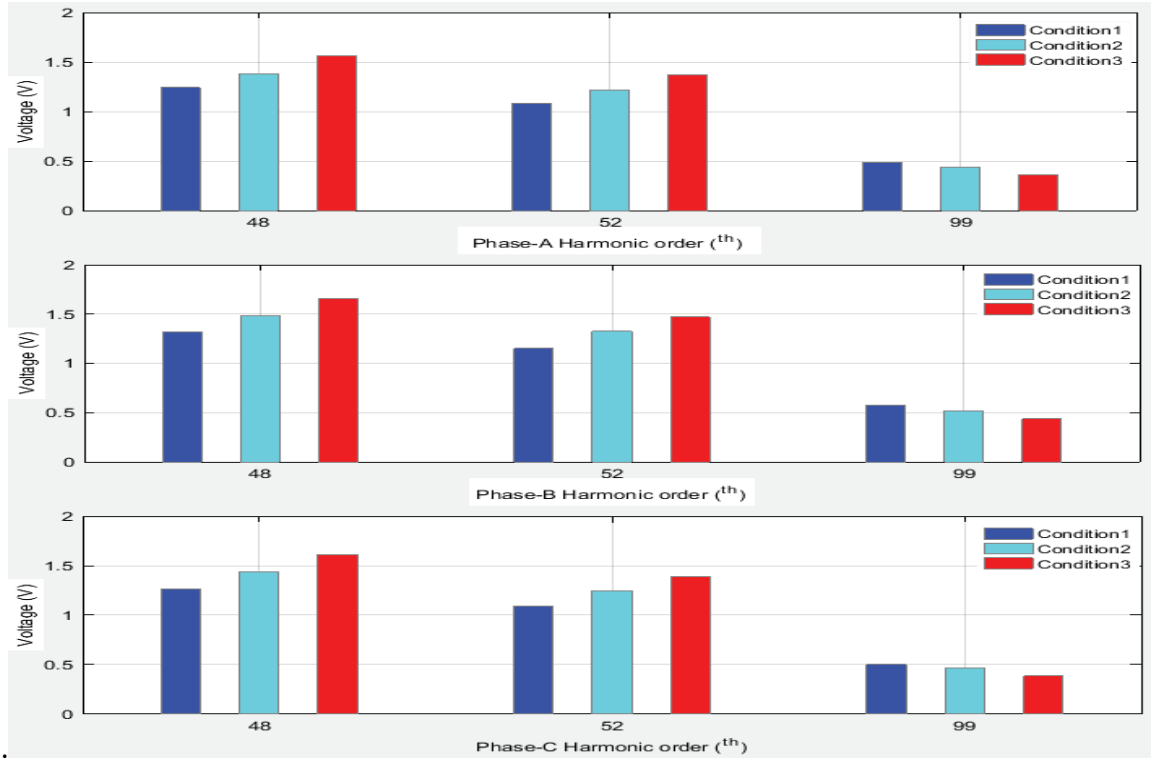


*Figure 11. Comparison of harmonic orders at different working condition*

## 5.0 DISCUSSION

When the inverter DC-side voltage varies, the fluctuation component of the voltage is transmitted to the AC side due to modulation, and an interharmonic generated on the AC side. For an inverter consisting of fully-controlled switching device, the DC-side voltage is usually kept constant under the action of a voltage-stabilizer control section, so that the PV inverter can be used without considering interharmonic presence. These harmonics generated by the inverters are injected into the power distribution systems at the point of common coupling (PCC) which potentially affects the customers connected to the same distribution systems [17].

However, for the doubly-fed wind turbine, the harmonic generation principle of the grid-side converter is similar to that of the direct-drive wind turbine, but due to the flux linkage of the rotor and stator of the doubly-fed wind turbine. The harmonics generated by the rotor-side converter also generate harmonics and interharmonics on the stator-side. Therefore, for the doubly-fed wind turbine, harmonics and interharmonic are mainly caused by two

factors: the grid-side converter and the rotor-side converter. In the doubly-fed wind turbine generation system, the interharmonics generated by the DC-side voltage fluctuations between the two converters can be ignored. However, the harmonics transmitted by the rotor-side converter generate harmonics that are transmitted to the stator-side through electromagnetic coupling cannot be ignored. The interharmonic frequency is related to the speed, carrier frequency, and the amplitude is related to the DC-side voltage, modulation index.

## 6.0 CONCLUSION

In this paper, the principles of harmonic and interharmonics generated by converters used in photovoltaic and wind turbine have been presented. Since both the photovoltaic and direct drive wind turbine are connected to the grid via the grid side converter, the interharmonic and harmonic generation principles of the two are generically cognate. While harmonic distortions are generated by dead zone effects of IGBT and PWM modulation, interharmonics are generated by DC side voltage of the inverter which is non-integer multiple of the fundamental frequency. Therefore, the harmonics and interharmonics generated by the inverters of the photovoltaic and direct drive wind turbine are mainly caused by three factors; videlicet PWM modulation, IGBT switch dead zone effect and DC voltage fluctuations.

## REFERENCES

K. Manickavasagam, N. K. Thotakanama, V. Puttaraj, "Intelligent energy management system for renewable energy driven ship", IET electrical system in transportation, vol. 9, pp. 24-34, 2019.

Wu, C., & Zhang, L. (2021). Utilization of Solar Energy for Ship Propulsion: A Review. IEEE Transactions on Sustainable Energy, 12(3), 1234-1248.

M. B. Anwar, M. S. El Moursi, and W. Xiao, "Dispatching and frequency control strategies for marine current turbines based on doubly fed induction generator", IEEE transaction on sustainable energy, vol. 7, pp. 262-270, 2016.

Gupta, S., & Singh, R. (2022, July). Performance Analysis of Wind Energy Systems for Ships. In Proceedings of the IEEE International Conference on Renewable Energy Applications in Maritime Transportation (REAMT), Singapore, pp. 123-128.

M. Johnson and A. Smith, "Harmonic Generation Analysis in PWM-Based Power Converters," IEEE Transactions on Power Electronics, vol. 45, no. 3, pp. 1234-1245, Mar. 2020.

A. Brown, B. Davis, and C. Wilson, "Mitigation of Harmonic Generation in PWM Inverters Using Active Filtering," Proceedings of the IEEE International Conference on Power Electronics and Energy Conversion Systems (PEECS), Sep. 2021, pp. 234-239.

C. L. Kuo, J. L. Chen, S. J. Chen, C. C. Kao, H. T. Yau, and C. H. Lin, "Photovoltaic energy conversion system detection using fractional-order color relation classifier

in micro distribution systems", IEEE transaction on smart grid., vol. 8, pp. 1163-1172, 2017.

M. R. Miyazaki, A. J. Sorensen, N. Lefebvre, K.K Yum and E. Pedersen, "Hybrid modeling of strategic loading of a marine hybrid power plant with experimental validation" IEEE Access, vol. 4, pp. 8793-8804, 2016.

M. Farbis, A. Hoevenaars, and M. McGraw, "Marine Duty Harmonic Mitigation on DC Propulsion Saves Oil Service Vessel Program", IEEE Tran. on industry applications, vol. 53, pp. 1617-1626, 2017.

B. Badrzadeh, and M. Gupta, "Practical Experiences and Mitigation Methods of Harmonics in Wind Power Plants", IEEE Tran. on industry applications, vol. 49, pp. 2279-2289, 2013.

M. Sharifzadeh, H. Vahedi, R. Portillo, L. G. Franquelo, and K. Al-Haddad, "Selective Harmonic Mitigation Based Self-Elimination of Triplen Harmonics for Single-Phase Five-Level Inverters", IEEE Tran. on power electronics, vol. 34, pp. 86-96, 2019.

J. Dai, S. W. Nam, M. Pande, G. Esmaeili, "Medium-voltage current source converter drives for marine propulsion system using a dual-winding synchronous machine", IEEE Tran. on industry applications, vol. 50, pp. 3971-3976, 2014.

M. Haring, E. Skjong, T. A. Johansen, and M. Molinas, "Extremum-seeking control for harmonic mitigation in electric grid of marine vessels", IEEE Trans. on industrial electronics, vol. 66, pp. 500-508, 2019.

J.M. Shen, H. L. Jou, J. C. Wu, and K. D. Wu, "Five-level inverter for renewable power generation system", IEEE transaction on energy conversion, vol. 28, pp. 257-267, 2013.

Adam Borowicz "GPU Implementation of Adaptive Fourier Decomposition" 2019 Signal Processing: Algorithms, Architectures, Arrangements, and Applications (SPA), IEEE Conference Paper Year: 2019, DOI: 10.23919/SPA.2019.8936752

J. Hou, Guangqian Ding, C. Wu;Z. Pan and J. Wang "An Interharmonic Suppression Control Scheme in PV System Based on DC-Link Voltage Perturbation Reduction" 2021 IEEE 5th Conference on Energy Internet and Energy System Integration (EI2), Year: 2021, DOI: 10.1109/EI252483.2021.9712976

J. H. R. Enslin and P. J. M. Heskes, "Harmonic interaction between a large number of distributed power inverters and the distribution network", IEEE transaction on power Electronics, vol. 19, pp. 1586-1593, 2004.